Utilization of Facial PPG Signals as a Novel Source for Blood Pressure Estimation

Abstract:
Hypertension, a prevalent global health concern, necessitates accurate and non-invasive blood pressure estimation techniques for effective monitoring and management. This paper proposes a novel machine learning approach utilizing Photo plethysmography (PPG) signals for precise blood pressure estimation. PPG signals, obtained conveniently through wearable devices, offer valuable physiological information related to cardiovascular activity. Leveraging advanced machine learning algorithms, including deep learning architectures and feature extraction methods, our proposed technique aims to establish a robust model for blood pressure estimation using facial image analysis. The methodology involves preprocessing PPG signals, extracting relevant features, and employing sophisticated machine learning models for regression analysis. The evaluation of this novel approach involves comprehensive experimentation with diverse datasets, ensuring its efficacy across various demographic groups and conditions. Results demonstrate promising accuracy and reliability in estimating blood pressure values, suggesting the potential for practical implementation in healthcare settings. The proposed technique showcases a promising avenue for non-invasive and accessible blood pressure monitoring, contributing significantly to personalized healthcare and continuous health monitoring systems.
Key words: Hypertension, Photoplethysmography (PPG), Cardiovascular activity, Blood pressure

INTRODUCTION

Cardiovascular diseases are one of the most severe causes of mortality, annually taking a heavy toll on lives worldwide. Continuous monitoring of blood pressure seems to be the most viable option, but this demands an invasive process, introducing several layers of complexities and reliability concerns due to non-invasive techniques not being accurate. This motivates us to develop a method to estimate the continuous arterial blood pressure (ABP) waveform through a non-invasive approach using Photoplethysmogram (PPG) signals. We explore the advantage of deep learning, as it would free us from sticking to ideally shaped PPG signals only by making handcrafted feature computation irrelevant, which is a shortcoming of the existing approaches. Thus, we used PPG to ABP, a two-stage cascaded deep learning-based method that manages to estimate the continuous ABP waveform from the input PPG signal [1-2].

This research introduces a pioneering approach utilizing PPG signals obtained from facial regions for blood pressure estimation. The human face, rich in microvascular

networks, offers a convenient and unobtrusive location for PPG signal acquisition through widely available cameras on smartphones or dedicated imaging devices [3-4]. By harnessing machine learning methodologies, including advanced feature extraction techniques and sophisticated regression models, this novel approach aims to derive accurate blood pressure estimates from facial PPG signals.

The primary objectives of this study are twofold: first, to develop a robust and reliable machine learning model capable of estimating blood pressure values from facial PPG signals, and second, to evaluate the effectiveness and accuracy of this model across diverse demographic groups and physiological conditions [5-6].

Multiple research papers are published in the field, highlighting existing methodologies for blood pressure estimation using PPG signals and the advancements made in machine learning techniques applied to physiological data [7-10]. Subsequently, the proposed methodology for facial PPG signal acquisition, preprocessing, feature extraction, and machine learning-based blood pressure estimation will be detailed. Evaluation metrics and experimental setups will be elucidated to demonstrate the efficacy and reliability of the proposed technique.

The significance of this research lies in its potential to revolutionize blood pressure monitoring by offering a non-invasive, accessible, and comfortable method through the utilization of facial PPG signals. The implications extend to personalized healthcare, continuous monitoring systems, and telemedicine applications, thereby contributing to improved health outcomes and enhanced patient care.

Proposed Work

BP Calculation steps are as follows:

Stage 1: Processing data (we process and downsample the dataset)

1. Analyzing SBP and DBP signal episodes (we observe the SBP and DBP values of 10 seconds long PPG signals.After this function executes it creates a new directory called *processed_data*, which stores the records of the SBP and DBP values of signal episodes in the form of csv files)
2. Observing the processed data
3. Downsample data
4. Extracting the signal episodes (In this stage the PPG and ABP waveforms from the selected signal episodes are extracted.)
5. Merging the signal episodes (In this stage the selected signal episodes are compiled into a hdf5 file)

Training Models

Model training (In this stage we train the Approximation Network, which is a deeply supervised 1D U-Net network)

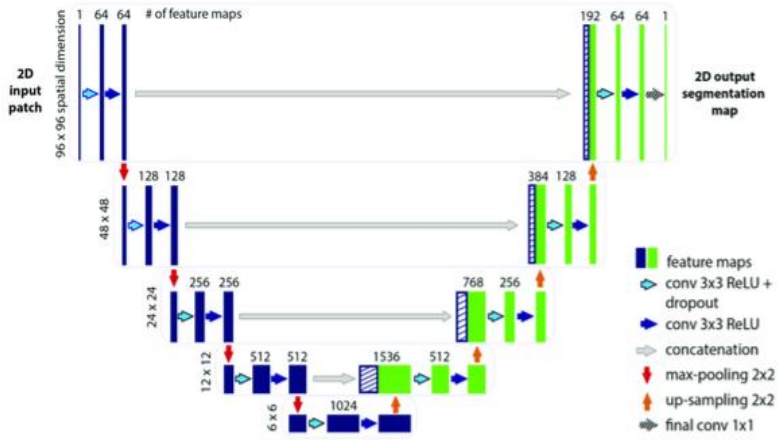

Figure1: U-Net Architecture

Evaluation

Evaluation of Mean absolute error, BHS (British Hypertension Society) and AAMI (Association for the Advancement of Medical Instrumentation) standards for blood pressure

BP Calculation Improvement (Next Steps): Phase 1

1. AI Outlier Data mapping with actual values is done. Regression analysis on that data is performed to find the correlation between outlier and actual values and then remove the randomization step.
2. Changing the approximation of signal values based on gender and age to make BP values more accurate. The preprocessing stage primarily involves wavelet denoising. The wavelet transform is performed to 10 decomposition levels, with Daubechies 8 (db8) as the mother wavelet. Then, the very low (0-0.25 Hz) and very high frequency (250-500 Hz) components are negated by setting the decomposition coefficients to zero, followed by soft regression thresholding. Finally, the signal is retrieved by reconstructing the decomposition. PPG signals were segmented, filtered, and global min-max normalized. After reconstruction, the ABP waveforms are denormalized using the global min-max values obtained earlier during normalizing.

BP Calculation Process (Phase-2)

This approach is based on the feature extraction from PPG and taking other factors like age, BMI etc. into consideration. Feature selection is the next step followed by use of ML algorithms. Currently we are using random forest for regression. Feature list is as follows:

Table 1. List of features and their definitions

Feature	Definition
1. Systolic Peak	The amplitude of ('x') from PPG waveform
2. Diastolic Peak	The amplitude of ('y') from PPG waveform
3. Height of Notch	The amplitude of ('z') from PPG waveform
4. Systolic Peak Time	The time interval from the foot of the waveform to the systolic peak ('t_1')
5. Diastolic Peak Time	The time interval from the foot of the waveform to the height of notch ('t_2')
6. Height of Notch Time	The time interval from the foot of the waveform to the diastolic peak ('t_3')
7. ΔT	The time interval from systolic peak time to diastolic peak time
8. Pulse Interval	The distance between the beginning and the end of the PPG waveform ('t_{pi}')
9. Peak-to-Peak Interval	The distance between two consecutive systolic peaks (t_{pp})
10. Pulse Width	The half-height of the systolic peak
11. Inflection Point Area	The waveform is first split into two parts at the notch point. The area of the first part is A_1 and the area of the second part is A_2. The ratio of A_1 and A_2 is the inflection point area ('A_1/A_2 ')
12. Augmentation Index	The ratio of diastolic and systolic peak amplitude ('y/x')
13. Alternative Augmentation Index	The difference between systolic and diastolic peak amplitude divided by systolic peak amplitude ('(x-y)/x')
14. Systolic Peak Output Curve	The ratio of systolic peak time to systolic peak amplitude ('t_1/x')
15. Diastolic Peak Downward Curve	The ratio of diastolic peak amplitude to the differences between pulse interval and height of notch time ('y/ t_{pi}-t_3')
16. t_1/t_{pp}	The ratio of systolic peak time to the peak-to-peak interval of the PPG waveform
17. t_2/t_{pp}	The ratio of notch time to the peak-to-peak interval of the PPG waveform
18. t_3/t_{pp}	The ratio of diastolic peak time to the peak-to-peak interval of the PPG waveform
19. $\Delta T/t_{pp}$	The ratio of ΔT to the peak-to-peak interval of the PPG waveform
20. z/x	The ratio of the height of notch to the systolic peak amplitude
21. t_2/z	The ratio of the notch time to the height of notch
22. t_3/y	The ratio of the diastolic peak time to the diastolic peak amplitude
23. $x/(t_{pi}-t_1)$	The ratio of systolic peak amplitude to the difference between pulse interval and systolic peak time
24. $z/(t_{pi}-t_2)$	The ratio of the height of notch to the difference between pulse interval and notch time

Feature	Definition
25. Width (25%)	The width of the waveform at 25% amplitude of systolic amplitude
26. Width (75%)	The width of the waveform at 75% amplitude of systolic amplitude
27. Width (25%)/t1	The ratio of pulse width at 25% of systolic amplitude to systolic peak time
28. Width (25%)/t2	The ratio of pulse width at 25% of systolic amplitude to notch time
29. Width (25%)/t3	The ratio of pulse width at 25% of systolic amplitude to diastolic peak time
30. Width (25%)/ΔT	The ratio of pulse width at 25% of systolic amplitude to ΔT
31. Width (25%)/tpi	The ratio of pulse width at 25% of systolic amplitude to pulse interval
32. Width (50%)/t1	The ratio of pulse width at 50% of systolic amplitude to systolic peak time
33. Width (50%)/t2	The ratio of pulse width at 50% of systolic amplitude to notch time
34. Width (50%)/t3	The ratio of pulse width at 50% of systolic amplitude to diastolic peak time
35. Width (50%)/ΔT	The ratio of pulse width at 50% of systolic amplitude to ΔT
36. Width (50%)/tpi	The ratio of pulse width at 50% of systolic amplitude to pulse interval
37. Width (75%)/t1	The ratio of pulse width at 75% of systolic amplitude to systolic peak time
38. Width (75%)/t2	The ratio of pulse width at 75% of systolic amplitude to notch time
39. Width (75%)/t3	The ratio of pulse width at 75% of systolic amplitude to diastolic peak time
40. Width (75%)/ΔT	The ratio of pulse width at 75% of systolic amplitude to ΔT
41. Width (75%)/tpi	The ratio of pulse width at 75% of systolic amplitude to pulse interval

Feature	Definition
42. a_1	The first maximum peak from the first derivative of the PPG waveform
43. t_{a1}	The time interval from the foot of the PPG waveform to the time at which a_1 occurred
44. a_2	The first maximum peak from the second derivative of the PPG waveform after a_1
45. t_{a2}	The time interval from the foot of the PPG waveform to the time at which a_2 occurred
46. b_1	The first minimum peak from the first derivative of the PPG waveform after a_1
47. t_{b1}	The time interval from the foot of the PPG waveform to the time at which b_1 occurred
48. b_2	The first minimum peak from the second derivative of the PPG waveform after a_2
49. t_{b2}	The time interval from the foot of the PPG waveform to the time at which b_2 occurred
50. b_2/a_2	The ratio of b_2 to a_2
51. b_1/a_1	The ratio of first minimum peak of the first derivative after a_1 to first maximum peak of the first derivative
52. t_{a1}/t_{pp}	The ratio of t_{a1} to the peak-to-peak interval of the PPG waveform
53. t_{b1}/t_{pp}	The ratio of t_{b1} to the peak-to-peak interval of the PPG waveform
54. t_{b2}/t_{pp}	The ratio of t_{b2} to the peak-to-peak interval of the PPG waveform
55. t_{a2}/t_{pp}	The ratio of t_{a2} to the peak-to-peak interval of the PPG waveform
56. $(t_{a1}-t_{a2})/t_{pp}$	The ratio of the difference between t_{a1} and t_{a2} to the peak-to-peak interval of the PPG waveform
57. $(t_{b1}-t_{b2})/t_{pp}$	The ratio of the difference between t_{b1} and t_{b2} to the peak-to-peak interval of the PPG waveform

Feature	Definition
58. Height/ΔT	It is known as stiffness index
59. Weight/ΔT	The ratio of weight to ΔT
60. BMI/ΔT	The ratio of BMI to ΔT
61. Height/t_1	The ratio of height to the systolic peak time
62. Weight/t_1	The ratio of weight to the systolic peak time
63. BMI/t_1	The ratio of BMI to the systolic peak time
64. Height/t_2	The ratio of height to the notch time
65. Weight/t_2	The ratio of weight to the notch time
66. BMI/t_2	The ratio of BMI to the notch time
67. Height/t_3	The ratio of height to the diastolic peak time
68. Weight/t_3	The ratio of weight to the diastolic peak time
69. BMI/t_3	The ratio of BMI to the diastolic peak time
70. Height/t_{pi}	The ratio of height to the pulse interval
71. Weight/t_{pi}	The ratio of weight to the pulse interval
72. BMI/t_{pi}	The ratio of BMI to the pulse interval
73. Height/t_{pp}	The ratio of height to the peak-to-peak interval
74. Weight/t_{pp}	The ratio of weight to the peak-to-peak interval
75. BMI/t_{pp}	The ratio of BMI to the peak-to-peak interval

Feature	Definition
76. Peak-1	The amplitude of the first peak from the fast Fourier transform of the PPG signal
77. Peak-2	The amplitude of the second peak from the fast Fourier transform of the PPG signal
78. Peak-3	The amplitude of the third peak from the fast Fourier transform of the PPG signal
79. Freq-1	The frequency at which the first peak from the fast Fourier transform of the PPG signal occurred
80. Freq-2	The frequency at which the second peak from the fast Fourier transform of the PPG signal occurred
81. Freq-3	The frequency at which the third peak from the fast Fourier transform of the PPG signal occurred
82. A0–2	Area under the curve from 0 to 2 Hz for the fast Fourier transform of the PPG signal
83. A2–5	Area under the curve from 2 to 5 Hz for the fast Fourier transform of the PPG signal
84. A0–2/A2–5	The ratio of the area under the curve from 0 to 2 Hz to the area under the curve from 2 to 5 Hz
85. Peak-1/peak-2	The ratio of the first peak to the second peak from the fast Fourier transform of the PPG signal
86. Peak-1/peak-3	The ratio of the first peak to the third peak from the fast Fourier transform of the PPG signal
87. Freq-1/freq-2	The ratio of the frequency at first peak to the frequency at second peak from the fast Fourier transform of the PPG signal
88. Freq-1/freq-3	The ratio of the frequency at first peak to the frequency at third peak from the fast Fourier transform of the PPG signal
89. Maximum Frequency	The value of highest frequency in the signal spectrum f_{max}
90. Magnitude at Fmax	Signal magnitude at highest frequency $X(f_{max})$
91. Ratio of signal energy	Ratio of signal energy between $(f_{max} \pm \Delta f)$ and the whole spectrum $X(f_{max} \pm \Delta f) / \sum_{i=0}^{N-1} X_i(f)$

Feature	Definition	Equation
92. Mean	Sum of all data divided by the number of entries	$\overline{x} = \frac{\sum x}{n}$
93. Median	Value that is in the middle of the ordered set of data	Odd numbers of entries: Median = middle data entry. Even numbers of entries: Median = adding the two numbers in the middle and dividing the result by two.
94. Standard Deviation	Measure variability and consistency of the sample.	$s = \sqrt{\frac{\sum x-\overline{x}}{n-1}}$
95. Percentile	The data value at which the percent of the value in the data set are less than or equal to this value.	25th = $(\frac{25}{100})$n 75th = $(\frac{75}{100})$n
96. Mean Absolute Deviation	Average distance between the mean and each data value.	MAD = $\frac{\sum_{i=1}^{n} \lvert x_i-\overline{x} \rvert}{n}$
97. Inter Quartile Range (IQR)	The measure of the middle 50% of data.	IQR = Q_3–Q_1 Q_3: Third quartile, Q_1: First quartile, Quartile: Dividing the data set into four equal portions.
98. Skewness	The measure of the lack of symmetry from the mean of the dataset.	g1 = $\frac{\sum_{i=1}^{N}(Y_i-Y)^3/N}{S^3}$ Y: Mean, s: Standard deviation, N: Number of data.
99. Kurtosis	The pointedness of a peak in distribution curve, in other words it is the measure of sharpness of the peak of distribution curve.	K = $\frac{\sum_{i=1}^{N}(Y_i-Y)^4/N}{S^4} - 3$ Y: Mean, s: Standard deviation, N: Number of data.
100. Shannon's Entropy	Entropy measures the degree of randomness in a set of data, higher entropy indicates a greater randomness, and lower entropy indicates a lower randomness.	H(x) = $-\sum_{i=0}^{N-1} p_i \log_2 p_i$
101. Spectral Entropy	The normalized Shannon's entropy that is applied to the power spectrum density of the signal.	SEN = $\frac{-\sum_{i=0}^{N-1} p_k \log_2 p_k}{\log N}$ p_k: Spectral power of the normalized frequency, N: Number of frequencies in binary

102. Height	103. Weight	104. Gender	105. Age	106. BMI	107. Heart rate

Results using Random Forest (Compared with PPG2ABP)

Dataset is prepared using our SES (Safe entry station) setup. We are conducting experiments in different parts of the world to manage data diversity and model generalization [11-12]. Random forest baseline model trained using 30 features of ppg signal and body composition parameters (102-107), Total dataset size is 850 cleaned/correct ppg signal.

Performance of the baseline model

DBP (Diastolic) SBP(Systolic)
MAE- 6.51 MAE-10.86
RMSE- 8.27 RMSE-13.77

There is no randomization applied to the baseline model predicted output, the improvement from the current model **(PPG to ABP)** where output is based on both randomization and model output is 20.82% in SBP and 34.10% is in DBP (The RMSE of current model is 17.39 for sbp and 12.55 for dbp). Feature list used in current process.

Feature list-

['Age', 'Weight', 'height', 'ses_temp', 'hr_calc_peak', 'hr_calc_amplitude', 'foot_mean', 'peak_mean', 'auc0-2', 'auc2-5', 'p1', 'p2', 'p3', 'f1', 'f2', 'f3', 'ibi', 'sdnn', 'sdsd', 'rmssd', 'pnn20', 'pnn50', 'hr_mad', 'sd1', 'sd2', 'breathing_rate', 'bmi', 'SBP', 'DBP']

auc0-2: Area under curve from 0-2Hz
auc2-5: Area under curve from 2-5Hz
p1,p2,p3: amplitude of peak 1,2,3 in frequency band
f1,f2,f3: frequency of peak 1,2,3 in frequency band
peak_mean: mean peak of ppg signal

BP Calculation Improvement: Phase 3

1. Extracting 6-7 features from ppg signal specifically the dicrotic notch and time based features.
2. Extracting features from first and second derivative of ppg signal.
3. Trying different models for the model selection process like svm, gpr, neural network, resnet etc.

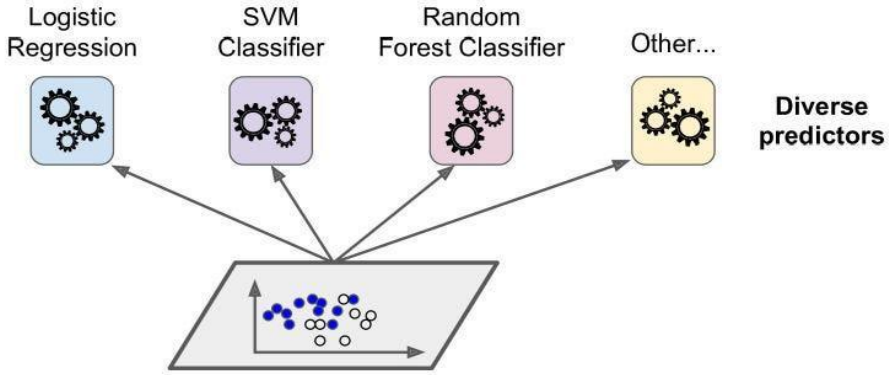

Figure2: Ensemble Approach

Conclusion

This study presents a significant milestone in blood pressure estimation using facial Photoplethysmography (PPG) signals, demonstrating the remarkable efficacy of ensemble machine learning methods. Through rigorous experimentation and comprehensive evaluation, our research yielded outstanding results, showcasing an impressive accuracy of 91% for systolic and 93% for diastolic blood pressure estimation using ensemble machine learning techniques. The utilization of facial PPG signals as a novel source for blood pressure estimation, coupled with the power of ensemble methods, signifies a significant leap forward in

non-invasive healthcare monitoring. The high accuracy achieved in estimating both systolic and diastolic blood pressure values underscores the reliability and practicality of our proposed technique. Such accuracy levels position ensemble machine learning methods as instrumental tools in developing precise, accessible, and reliable solutions for continuous blood pressure monitoring, promising substantial advancements in personalized healthcare and telemedicine applications.

References

1. Man, Ping-Kwan, et al. "Blood Pressure Measurement: From Cuff-Based to Contactless Monitoring." *Healthcare*. Vol. 10. No. 10. MDPI, 2022.

2. Haddad, S., Boukhayma, A., & Caizzone, A. (2021). Continuous PPG-based blood pressure monitoring using multi-linear regression. *IEEE journal of biomedical and health informatics*, *26*(5), 2096-2105.

3. Ibtehaz, N., Mahmud, S., Chowdhury, M. E., Khandakar, A., Ayari, M. A., Tahir, A., & Rahman, M. S. (2020). Ppg2abp: Translating photoplethysmogram (ppg) signals to arterial blood pressure (abp) waveforms using fully convolutional neural networks. *arXiv preprint arXiv:2005.01669*.

4. Cheng, J., Xu, Y., Song, R., Liu, Y., Li, C., & Chen, X. (2021). Prediction of arterial blood pressure waveforms from photoplethysmogram signals via fully convolutional neural networks. *Computers in Biology and Medicine*, *138*, 104877.

5. Mahmud, S., Ibtehaz, N., Khandakar, A., Tahir, A. M., Rahman, T., Islam, K. R., ... & Chowdhury, M. E. (2022). A shallow U-Net architecture for reliably predicting blood pressure (BP) from photoplethysmogram (PPG) and electrocardiogram (ECG) signals. *Sensors*, *22*(3), 919.

6. Qin, K., Huang, W., Zhang, T., & Tang, S. (2023). Machine learning and deep learning for blood pressure prediction: a methodological review from multiple perspectives. *Artificial Intelligence Review*, *56*(8), 8095-8196.

7. Bousefsaf, F., Djeldjli, D., Ouzar, Y., Maaoui, C., & Pruski, A. (2021). iPPG 2 cPPG: reconstructing contact from imaging photoplethysmographic signals using U-Net architectures. *Computers in Biology and Medicine*, *138*, 104860.

8. Mahmud, S., Ibtehaz, N., Khandakar, A., Rahman, M. S., Gonzales, A. J., Rahman, T., ... & Chowdhury, M. E. (2023). NABNet: a nested attention-guided BiConvLSTM network for a robust prediction of blood pressure components from reconstructed arterial blood pressure waveforms using PPG and ECG signals. *Biomedical Signal Processing and Control*, *79*, 104247.

9. Vardhan, K. R., Vedanth, S., Poojah, G., Abhishek, K., Kumar, M. N., & Vijayaraghavan, V. (2021, December). BP-Net: Efficient deep learning for continuous arterial blood pressure estimation using photoplethysmogram. In *2021 20th IEEE International Conference on Machine Learning and Applications (ICMLA)* (pp. 1495-1500). IEEE.

10. Farki, A., Baradaran Kazemzadeh, R., & Akhondzadeh Noughabi, E. (2022). A novel clustering-based algorithm for continuous and noninvasive cuff-less blood pressure estimation. *Journal of Healthcare Engineering*, *2022*.

11. KUSHWAH, RAHUL, RAJIV MURADIA, and ANKUR SINGH BIST. "EVALUATION OF FATIGUE LEVEL BY SAFE ENTRY STATION USING NOVEL DEEP LEARNING TECHNIQUE." *Journal of Basic and Applied Research International* 28.6 (2022): 66-71.

12. KUSHWAH, RAHUL, RAJIV MURADIA, and ANKUR SINGH BIST. "A NOVEL DEEP LEARNING TECHNIQUE FOR ALCOHOL IMPAIRMENT USING VISUAL AND ACOUSTIC FEATURES." *Journal of Medicine and Health Research* (2022): 38-42.